MSC-IN-EG-65-25

PROJECT APOLLO

SIMULATION STUDY OF THE POWERED DESCENT PHASE OF THE LEM MISSION FROM TRANSITION TO TOUCHDOWN

Prepared by: _____
Richard Reid

and

_____
Herbert G. Patterson

Approved by: _____
David W. Gilbert
Chief, Engineering Simulation Br.

Approved by: _____
Robert G. Chilton
Deputy Chief
Guidance and Control Division

NATIONAL AERONAUTICS AND SPACE ADMINISTRATION
MANNED SPACECRAFT CENTER
Houston, Texas

June 15, 1965

LIST OF TABLES

TABLE OF CONTENTS

LIST OF FIGURES

SUMMARY

The powered descent phase of the LEM mission from transition to touchdown was studied utilizing facilities assigned to the Guidance and Control Division. A fixed-base simulator containing an attitude hand controller, descent engine throttle, and pilot displays was used to represent Lunar Excursion Module (LEM). The six-degrees-of-freedom equations of motion were solved utilizing analog computing equipment. The main areas under study during the simulation were:

1. Three rate of descent control modes proposed for use in the LEM spacecraft and

2. A modified (zero-overshoot) rate command-attitude hold (RCAH) control mode.

Results of the simulation indicate that the rate of descent control mode having a discrete level rate of descent is of considerable aid in reducing task loading and providing ease of control during landing maneuver. Also, a rate command-attitude hold (RCAH) control system, where the attitude hold is engaged after attitude rates are less than 2 degrees/second, does not degrade the handling qualities of the LEM attitude control system.

INTRODUCTION

The control problems associated with the LEM spacecraft during the final phases of the lunar landing mission have been examined in a number of previous piloted simulation studies conducted by the Guidance and Control Division. The studies documented in references 1 and 2 examined variations in the characteristic parameters of the attitude control system such as thruster size, time constant, damping ratio, natural frequency, and control sensitivity to determine their effect on pilot rating.

Reference 3 presents the preliminary analysis of the test data obtained from an analog simulation study to determine limits of pilot controlled landing touchdown velocities of the LEM spacecraft.

Previous simulations of the lunar landing maneuver have indicated the probable velocity limits of the pilot controlled LEM landing (reference 3). However, the lunar landing control task is one requiring proper coordination of throttle and attitude and monitoring of altitude rate meter to prevent the descent rate from building up over a period of time to relatively unsafe magnitudes. A second piloting problem associated with the LEM spacecraft, which became apparent in later lunar landing simulations, results from engaging the control system attitude hold feature immediately after the rotational controller has been placed in

the detent position. If relatively high angular rates have been used for attitude maneuvering, considerable overshoot of the commanded attitude occurs because of the low control power. This makes accurate attitude maneuvers by the pilot difficult and has an undesirable effect on attitude fuel consumption.

There are several possible methods for implementing a rate of descent mode and to correct the overshoot problem of the rate command-attitude hold control mode. To determine the feasibility of implementing these methods in the LEM spacecraft, the Guidance and Control Division conducted a piloted simulation study of the lunar landing phase of the LEM mission. The objectives of this simulation study were to:

1. Evaluate three types of rate of descent command options and

2. Evaluate a method for correcting the overshoot of commanded attitude in rate command-attitude hold control mode.

LIST OF SYMBOLS

a_1 , a_2 , a_3 b_1 , b_2 , b_3 c_1 , c_2 , c_3	Direction cosines ("I" frame to "G" frame)
a_x , a_y , a_z	Acceleration along the X_b , Y_b , Y_b axes, ft/sec
C_1 , C_2	Gains in the rate-of-descent control modes
c.g.	Center of gravity
g_m	Lunar gravitational acceleration, ft/sec^2
h	Altitude, ft
I_X , I_Y , I_Z	Roll, pitch, and yaw moments of inertia, slug - ft^2
I_{XY}, I_{XZ}, I_{YZ}	Products of inertia in the X_b- Y_b, X_b- Z_b, and Y_b- Z_b plane, slug - ft^2
K	Ratio of rate to altitude feedback, deg/deg
$K_1 \rightarrow K_{13}$	Arbitrary constants
L	Lunar latitude, deg
L, M, N	Applied roll, pitch, and yaw moments, ft-lb
l_{XY}	Characteristic jet damping distance parallel to X_b- Y_b plane, ft
l_Z	Distance from c.g. to main engine nozzle exit along Z_b, ft

l_1 , l_2 , l_3 m_1 , m_2 , m_3 n_1 , n_2 , n_3	Direction cosines ("I" frame to "B" frame)
M_ϕ , M_θ , M_ψ	RCS roll, pitch, and yaw moments, ft-lb
m_m	Mass used of main engine fuel, slugs
m_{RCS}	Mass used of RCS fuel, slugs
W_{RCS}	Weight used of RCS fuel, lb
m_T	Total mass of spacecraft, slugs
OL	Open Loop
p, q, r	Roll, pitch, and yaw rates, rad/sec
R_m	Lunar radius, ft
R_T	Range, ft
S	Laplace operator
T_m	Main engine thrust, lb
t	Time, sec
u, v, w	Velocities along X_b, Y_b, Z_b, ft/sec
u_{r_1}, v_{r_1}, w_{r_1}	Radar position (1) velocities, ft/sec
u_{r_2}, v_{r_2}, w_{r_2}	Radar position (2) velocities, ft/sec
Δ V	Characteristic velocity, ft/sec

V_{X_D}, V_{Y_D}, V_{Z_D}	Inertial display velocities, ft/sec
V_{X_G}, V_{Y_G}, V_{Z_G}	Velocities along X_G, Y_G, Z_G ft/sec
V_{X_I}, V_{Y_I}, V_{Z_I}	Velocities along X_I, Y_I, Z_I ft/sec
X_b, Y_b, Z_b	Coordinates of the "B" frame
X_G, Y_G, Z_G	Coordinates in the "G" frame
X_I, Y_I, Z_I	Coordinates in the "I" frame
X_r, Y_r, Z_r	Coordinates in the "r" frame
X_1	Distance from "B" frame origin to c.g. along X_b, ft
Y_1	Distance from "B" frame origin to c.g. along Y_b, ft
Z_1	Distance from c.g. to main engine gimbal in the Z_b direction, ft
δ_T	Throttle deflection, deg
δ_θ, δ_ϕ	Pitch and roll trim gimbal position, rad
ϵ	Control Error Signal
λ	Lunar longitude, deg
θ, ψ, ϕ	Spacecraft angular position, rad
θ_c	Commanded pitch angle, deg
σ	Standard deviation
σ_R	Radar transformation angle, rad

ω	Angular frequency, rad/sec
$\dot{}$	A dot over a quantity represents the first derivative with respect to time
(0)	A variable quantity at time zero
(t)	A variable quantity at time t

VEHICLE SIMULATION

The LEM spacecraft powered descent study was implemented by coupling an analog computer solution of the spacecraft equation of motion to a fixed-base partial simulation of the LEM cockpit.

Characteristics of Simulated Vehicle

The general configuration of the simulated LEM vehicle is shown in figure 1. The initial conditions assumed for the physical parameters of the LEM spacecraft were:

Quantity	Symbol Value
Mass, slugs	$M_T = 468.15$
Roll inertia, slug - ft^2	$I_X = 13084$
Pitch inertia, slug - ft	$I_Y = 10779$
Yaw inertia, slug - ft	$I_Z = 10990$
Product of inertia in the X_b-Z_b plane, slug - ft^2	$I_{XZ} = -313$
Product of inertia in the X_b-Y_b plane, slug - ft^2	$I_{XY} = -42$
Product of inertia in the Y_b Z_b plane, slug - ft^2	$I_{YZ} = -190$
Distance from origin to c.g. along X_b, ft	$X_1 = 0$
Distance from origin to c.g. along Y_b, ft	$X_1 = .145$
Distance from c.g. to main engine gimbal in the Z_b direction, ft	$Z_1 = 4.45$
Distance from c.g. to main engine exit along Z_b, ft	$l_Z = 5.514$
Characteristic jet damping distance parallel to X_b-Y_b plane, ft	$l_{XY} = 3.91$

These quantities varied as a function of mass and changed according to the equations in Appendix A.

Equations of Motion

The equations of motion were written in six-degrees-of-freedom which represent summations of forces and moments along and about the three spacecraft body axes (X_b, Y_b, Z_b). A right-handed system or orthogonal coordinate axes was fixed to the moon model (figure 2). The moon model was considered to be non-rotational and therefore this axis system can be considered to be an inertial system. The Y_I axis was positive along the positive rotational axes of the moon, the negative X_I axis was through the desired target on the moon equator, and the Z_I axis completed the right-handed coordinate system. The third orthogonal axis system was located on the moon model surface and lies on a line connecting the vehicle and the center of the moon model (figure 2). The positive Y_G axis was pointed toward the lunar West parallel to the plane of the moon equator and the positive Z_G axis was through the center of the moon model.

The spacecraft attitude angles between inertial and spacecraft axes (order of rotation θ, Ψ , ϕ) represent the angular orientation of the spacecraft. The equations of motion for the spherical nonrotating moon model are presented in Appendix A.

Control System

The attitude control was provided for three modes of operation:

1. Rate command-attitude hold (RCAH),
2. Rate command (RC), and
3. Direct thruster operation.

The linear pulse ratio modulation used in the RCAH and RC modes was generated from a jet select modulator and logic box. In addition, a constant speed two-axis gimbal was assumed for automatic trim of the main engine thrust vector through the varying center of gravity location.

Trim Gimbal.-The actual c.g. offset from the main engine thrust vector produces moments about the pitch and roll body axes of the spacecraft which, in turn, produce steady state error signals in the pitch and roll control axes. To automatically realine the thrust vector through the c.g., these error signals are used to actuate the drive motors of the trim gimbal system (for error signals greater than 0.1 degree) at a constant speed of ± 0.2 degree/second. The maximum gimbal angles are ± 6.0 degrees. In the study, the trim gimbal system was simulated by a descent engine control assembly (DECA) box built by the Guidance and Control Division.

Rate of Descent (ROD) Command.-The mechanization of the rate of descent modes used during the study are shown in figure 3. The ROD was commanded through the descent engine throttle and/or through a two position center-off switch located on the throttle housing. The ROD command modes were activated when the attitude control switch was in RCAH position and the thrust control switch in the AUTO position, but were automatically switched to direct engine thrust control whenever the throttle deflection exceeded 51° (throttle soft stop location). The four ROD command modes investigated in the study are presented in block diagram form in figure 4. The values of the feedback gains (C_1 and C_2) used in the different congigurations are contained in table 1. As indicated in figure 4, mode 1 had no altitude rate feedback and thus the throttle setting controlled the thrust directly. Mode 2 had linear altitude rate feedback; mode 3 used nonlinear altitude rate feedback; and mode 4 had a linear, high gain altitude rate feedback and used the toggle switch mentioned previously to change the ROD in increments of 2 feet/second/pulse. The throttle servo and engine thrust mechanization shown in figure 4 represents the engine thrust characteristics of the LEM.

Rate command-attitude hold (RCAH).-The pitch attitude control system used in the simulation is shown in figure 4. The circuitry for the roll and yaw channels was identical except that the yaw axis error signal was not connected to the trim gimbal. The detent switches switched the mode of the attitude follower circuit so that the output of the follower either followed the input signal or held the last value of the input signal. This system also included an inhibition circuit which prevented the follower circuit from holding the last value of the input signal until the sum of the absolute value of vehicle attitude rates were below a preselected magnitude; i.e., $|p| + |q| + |r| \leq 1$, 2, 3, or 5 degrees/second. The simulation was simplified in that transformation of attitude error signal to the proper body axis rate command was neglected. Large roll and yaw angles were avoided during the simulation so the effect was considered negligible.

Simulator Cockpit

The simulator cockpit used in the study consisted of the astronaut chairs, attitude controller, throttle, and spacecraft display panel enclosed in a partial mockup of the LEM spacecraft cabin.

Astronaut chairs.-The actual spacecraft has a harness-type arrangement to restrain the pilots, but chairs were used in this simulation for pilot comfort. However, the chairs were positioned so that the window view angle was the same as the harness arrangement.

Attitude controller.-The attitude controller used to actuate the attitude jets was a three-axis hand controller of the Gemini type (figure 5) having a maximum deflection of $\pm$10 degrees in any direction. The controller was

spring loaded so that if no force was applied, the handle returned to the zero position. Movements of the controller in the pitch direction (forward or back) were about a pivot point located approximately halfway up the handle. Yaw maneuvers were performed by movement of the controller (turned right and left) about the controller longitudinal axis. Roll maneuvers were performed by movements of the controller (right and left) about a pivot point at the base of the controller. The physical characteristics of the controller used were:

Maneuver	Break-out Moment	Moment at Maximum Deflection
Roll	3 in-lb	9 in-lb
Pitch	5 in-lb	23 in-lb
Yaw	6.5 in-lb	14 in-lb

Throttle.-The throttle used in the simulation was a duplicate of the proposed LEM throttle as of August 15, 1963 (figure 6). A single linear potentiometer controlled the output voltage for the throttle and full throttle angular range was from 0° to 66°. There was a soft stop at 51° which indicated to the pilots the throttle deflection point where the ROD command mode was disengaged.

Spacecraft display panel.-A photograph of the spacecraft display panel used in the simulation is presented in figure 7. The instruments shown on the panel are (1) forward and lateral velocity, (2)ΔV, (3) % fuel remaining, (4) % thrust, (5) FDAI, (6) altitude, (7) altitude rate, (8) T/W ratio, (9) downrange distance to the center of the target, and (10) a clock for indicating elapsed time of flight. The forward and lateral velocity, altitude, altitude rate, and downrange distance were all nonlinear meters having logarithmic scales. This eliminated scale change requirements and maintained a fairly good resolution at near zero values. The forward and lateral velocity resolution near zero was approximately ± 0.5 fps, the altitude resolution was ± 1 ft., and the altitude rate approximately ± 0.25 fps. The downrange meter, which was only used at large distances because the out-the-window display was used closer to touchdown, had a resolution of approximately ± 10 feet. The FDAI in the actual LEM displays the output of the Gimbal Attitude Servo Transformation Assembly (GASTA) which in turn is driven by the gimbal angles of the inertial platform. In the simulation, the FDAI was driven by the spacecraft angular position angles θ, ψ, and ϕ. The platform was alined with the target point so that zero reading of the FDAI at the target point indicated that spacecraft X_b axis was alined with the local horizontal and pointed along the lunar equator in the negative direction of the moon rotation. Also, for a zero FDAI reading at the target point, Y_b was in the direction of the positive moon rotation axis and Z_b was directed toward the center of the moon. A zero FDAI reading (ψ, θ, $\phi = 0$) at the target meant that the body axis was alined with the inertial axes.

Out-the-Window Display

The out-the-window display was generated by the Visual Space Flight Simulator which is an electronic system designed to simulate the visual environment of a space vehicle. The display consists of special purpose digital units and specially designed television display units. The digital units accept numerical data describing the position and attitude of the vehicle and perform the computation necessary to produce the appropriate perspective pictures of the environment of the spacecraft with respect to the generated plane (lunar surface). The display units use the results of the computation to produce color pictures on shadow mask television cathode ray tubes which are presented to the pilot through an optical system in the form of a virtual image. The landing site, as established in this study, was 512 feet square and consisted of green and yellow checkerboard squares having an area of 16 feet on a side. The target area was centered in a blue and red area 2,048 feet square having squares of various sizes. The rest of the plane consisted of a repetitive green and yellow pattern.

TEST PROCEDURES

Initial Conditions

The simulation started with the spacecraft at a transition altitude of 1,200 feet. The target had an inertial position of $X_I = Y_I = Z_I = 0$. The spacecraft was in an equatorial lunar plane. The initial conditions of the simulation were as follows:

Parameter	Number	Units
t	0	sec
V_{X_I}	-155	ft/sec
V_{Y_I}	0	ft/sec
V_{Z_I}	42	ft/sec
X_I	-4,465	ft
Y_I	0	ft
Z_I	-1,200	ft
λ	-.464	deg
L	0	deg
h	1,200	ft
θ	41.4	deg
	0	deg

Parameter	Number	Units
ϕ	0	deg
p	0	deg/sec
q	0	deg/sec
r	0	deg/sec
M	383.61	slugs
M_T	468.15	slugs
I_X	13,082	slug-ft^2
I_Y	10,779	slug-ft^2
I_Z	10,990	slug-ft^2
I_{XY}	-313	slug-ft^2
I_{XZ}	-42	slug-ft^2
I_{YZ}	-190	slug-ft^2
X_1	0	ft
Y_1	-.145	ft
Z_1	4.45	ft
Z	5.514	ft
XY	3.91	ft
δ_θ	0	deg
δ_ϕ	0	deg
T	4,330	lb

Landing Technique

The landing technique used during the simulation was for the pilot to take manual control at an altitude of 750 feet. At this altitude, pitch attitude was 42° pitchback, forward velocity was 110 feet/second, and the descent rate near -22 feet/second. Range to the landing site was roughly 3,400 feet. The landing procedure used was as follows:

1. The throttle was set at T/W ratio of 1.3 and the control mode was changed from AUTO to RCAH. The vehicle was then pitched forward to about 10° pitchback. At this time, the forward velocity was about 60 feet/second, the descent rate -15 feet/second, and the range to the landing site 2,700 feet.

2. The 10° pitchback attitude was maintained until forward velocity was reduced to about 35 feet/second. During this period, the descent rate was gradually reduced to about -10 feet/second. The vehicle was pitched forward to a vertical attitude after the velocity had been reduced to the 35 feet/second value.

3. When the pilot decided from the visual display information that forward velocity could be nulled near the center of the target, the spacecraft was pitched back to an angle between 10° and 15°. If the spacecraft was not in the target area when the forward velocity was nulled, the spacecraft was pitched forward to gain velocity and then pitched back and stopped when above the estimated target center. If the target area was reached but the spacecraft was not in the center when the forward velocity could be nulled near the center of the target, the pilots were instructed to land at that point.

4. The rate of descent schedule used in reaching the landing area was to maintain approximately

a. 10 feet/second,
b. 8 feet/second from 200 feet to 100 feet altitude,
c. 6 feet/second from 100 feet to 50 feet, and 4 feet/second during the final vertical descent from 50 feet.

The descent engine was shut down when the probe light indicated the landing gear pads were 3 feet above the surface. Instructions to the pilots were to land with the forward and lateral translational velocities as near zero as possible. An upper limit on vertical velocity was not set, but the descent rate at engine shutoff was to be near 4 feet/second. There was no attempt made to bring the spacecraft to a zero rate of descent before the descent engine was cut off.

Recorded Data

The following flight parameters were recorded as a function of time during the simulation:

Flight Channel Recorder (A).-

M_M	Main engine fuel, lb
W_{RCS}	RCA fuel, lb
ΔV	Characteristic velocity, ft/sec

M_θ	RCS pitch moment, ft-lb
M_ψ	RCS yaw moment, ft-lb
M_ϕ	RCS roll moment, ft-lb
δ_θ	Trim gimbal (pitch), deg
δ_ϕ	Trim gimbal (roll), deg

Eight Channel Recorder (B).-

V_{XI}	Velocity along X_I, ft/sec
V_{YI}	Velocity along Y_I, ft/sec
V_{ZI}	Velocity along Z_I, ft/sec
p	roll rate, deg/sec
q	pitch rate, deg/sec
r	yaw rate, deg/sec
$T_m/M_T g_m$	Thrust to weight, lb/lunar wt.
$\dot{h}$	Altitude rate, ft/sec

X-Y Plotter (1)

h vs X_I

The following flight parameters were recorded at the end of each flight.

X_I	Displacement along X_I, ft
Y_I	Displacement along Y_I, ft
Z_I	Displacement along Z_I, ft
V_{XI}	Velocity along X_I, ft/sec
V_{YI}	Velocity along Y_I, ft/sec
V_{ZI}	Velocity along Z_I, ft/sec
p	roll rate, deg/sec
q	pitch rate, deg/sec
r	yaw rate, deg/sec

t	Time, sec
M_M	Main engine fuel, slugs
W_{RCS}	RCS fuel, lb
ΔV	Characteristic velocity, ft/sec
θ, Ψ, ϕ	spacecraft angular position, deg

TEST SCHEDULE

The test schedule used during the simulation study:

TEST CASE	PURPOSE
1. Rate of Descent Control	Evaluate pilot ability to control landing using: a. Direct Control of Descent Engine Thrust b. Linear rate feedback ROD control mode c. Nonlinear rate feedback ROD control mode d. Incremental (discrete level) ROD control mode
2. Attitude Hold Engage	Evaluate handling qualities of the LEM spacecraft with the following: a. Sum of absolute values of all angular rates less than 5 degrees/second before attitude hold command is activated. b. Same as a except rates 3 deg/sec c. Same as a except rates 2 deg/sec d. Same as a except rates 1 deg/sec

RESULTS AND DISCUSSION

The data taken to evaluate the rate of descent modes was from 5 test subjects who flew each of the four modes 5 times with the exception of mode 4, which was flown by only 4 subjects. The evaluation was divided into pilot opinion of the different control modes using the Cooper rating scale and vehicle end conditions at touchdown. The end conditions were further divided into task parameters (those parameters which were to be within a specified value at touchdown) and non-task parameters (those in which a particular value was not a task). The task parameters were: forward and lateral position, forward and lateral, and vertical velocities, the three spacecraft body angles (θ, Ψ , ϕ), and the spacecraft angular rates. The non-task rates were: time, Δ V, and weight of RCS and main engine fuel. The zero overshoot RCAH evaluation was by pilot opinion using the Cooper rating scale.

Rate of Descent Commands

Pilot opinion.-The results of the pilot evaluation indicated all ROD mechanizations had satisfactory handling qualities except the direct thrust mode. As shown in table 2, the mode receiving the test rating was the incremental mode, and in descending order the nonlinear and linear feedback modes, and the least preferable, the direct mode. The direct thrust mode was rated slightly less than satisfactory (4.1). The reason for this rating was because the control task required proper coordination of throttle and attitude and fairly intensive monitoring of altitude rate to prevent the descent rate from building up over a period of time to relatively unsafe magnitudes. Most pilots tended to rate the linear and nonlinear feedback mechanizations very nearly the same (3.0 and 3.2 respectively), although the response of the nonlinear feedback was rated somewhat better for the final descent maneuver. However, both these systems required attention to set and maintain the rate of descent at a given value because the pilot did not know the relationship between throttle setting and rate of descent. Thus, every time the throttle was moved to change the rate of descent, the pilot was required to observe the altitude rate meter to accurately set the desired rate of descent. The incremental mode received the highest rating (1.6) because it required very little attention once an initial descent rate had been set up. In this mode, the pilot simply counted the pulses to quickly determine the new rate of descent thereby providing him more time to devote to other tasks.

End conditions at touchdown.-The mean and 3 σ values of recorded end conditions for all the subjects combined is shown in tables 3 and 4, for task and non-task parameters respectively. The 3 σ values represent deviations about the mean with normal distribution assumed. These tables show that the individual parameters of the different modes have very nearly the same mean values and there is little indication

that one system is superior to another. In addition, all the mean values are within acceptable limits. When the 3σ values for task parameters are included in the evaluation, a definite trend of control system performance appears. In table 3, the dispersion of touchdown velocities decreased from the greatest for mode 1 to the least for mode 4. The other parameters of table 3, although not as consistent as the velocities, also show the same trend. Table 4 shows both the mean and 3σ values for each mode to be very close and thus it is difficult to readily conclude that one control system is superior to the other. The extremely large 3σ value of (1.77 deg/sec) shown for pitch attitude rate in mode two was caused by one pilot landing with pitch rate of 2.96 deg/sec. Examination of the end condition data shows all other pitch rates at touchdown to be less than 0.20 deg/sec.

End condition analysis.-To assist in analyzing the end conditions, a grading system was devised which scored each control mode on the basis of the |mean| and 3σ values of each parameter. For each parameter, the mode having the largest |mean| $+3\sigma$ value was given a 4 for that parameter and the mode with the smallest |mean| $+3\sigma$ was given a 1. The grade for a given control mode was the sum of the grades for the separate parameters. The lowest grade, and therefore the best control mode, was the mode having the parameters with the smallest |mean| $+ 3\sigma$. Because there is very little difference in the three body rates and main engine fuel, these parameters were deleted in the grading system. However, including these numbers would not appreciably change the results.

The results of the grading system for task (table 5) show that the incremental mode (mode 4) was superior to the other 3 modes. Modes 2 and 3 did provide an improvement over mode 1, but mode 4 showed twice as much improvement over mode 1 as did modes 2 and 3. There is good correlation between the task parameter grading system and pilot grading. This is expected because in the lunar landing maneuver, rate of descent control is of prime importance and requires close attention by the pilot and, with the addition of the ROD control mode, the pilot has more time for monitoring and correcting other parameters.

The non-task parameter ratings show that mode 1 is best with mode 4 almost as good. There is more significant decrease in rating (large number) for modes 2 and 3 with 2 slightly better than 3. These results are based on very little difference in the data for the non-task parameters and therefore the grading system may not be as significant as for the task parameters. The difference in ratings are most likely a result of modes 2 and 3 requiring a movement of the throttle and waiting to see the change in rate of descent. In many cases, this resulted in over correcting (reducing the rate of descent to zero or even a positive value) and using excess time and Δ V and requiring more attitude corrections. Overall, the data indicate little improvement for modes 2 and 3 with considerable improvement in mode 4.

Mode 4 had two significant system advantages over modes 2 and 3. First, the incremental input gave the pilot a definite indication of how much change in descent rate he was commanding and second, it had a system response that was approximately three times as fast. This latter advantage is an artificial one resulting from the ground rule that no changes to the existing throttle control circuitry were permitted. With this rule, the only way to get a fast system response is to use a high gain descent rate feedback signal but with the existing throttle output signal gain, the command range of descent rate available would have been too limited. Hence, the modes that used the existing throttle as the command input device for descent rate had to use an appropriately low feedback gain. Since the incremental command mode required a new input device anyway, it was selected to have a gain compatible with the desired feedback gain thus resulting in a faster system response.

Evaluation of the Modified RCAH Mode

The procedure used for evaluation was to fly the landing maneuver described in the previous section. The attitude hold feature was engaged at $|p| + |q| + |r| \leq 1$, 2, 3, or 5 degrees/second attitude rate. The test subjects flew the RCAH mode for each engagement rate and rated the system according to the Cooper rating scale. The results of the pilot evaluation (table 6) indicated no significant difference in system response for rate thresholds of less than 2 degrees/second. Engagement of the attitude hold feature at a rate threshold of 3 degrees/second and greater caused the pilots to complain that the overshoot was noticeable enough to be distracting. As shown in table 6, averaging of the various pilot ratings indicates the breakpoint for satisfactory handling qualities is about 2 degrees/second.

CONCLUDING REMARKS

1. The incremental rate of descent mode reduces the task loading considerably with very little effect of non-task parameters.

2. Attitude hold engagement rates of less than or equal to 2 degrees/second provides rate command attitude control mode having satisfactory handling qualities.

3. The addition of a rate-of-descent mode decreased the velocity dispersions at touchdown when incorporated into the simulation.

4. Task loading is reduced with the addition of a rate of descent mode.

REFERENCES

1. NASA Project Apollo Working Paper No. 1074, "Study of the Attitude Control Handling Qualities of the LEM During the Final Approach to Lunar Landing," by Donald C. Cheatham and Thomas E. Moore, dated May 10, 1963.

2. NASA Project Apollo Working Paper No. 1088, "A Simulation Study of the Landing - Approach Attitude Control Handling Qualities of the LEM Using On-Off RCS Thruster Logic," by William Stubblefield, et al, dated August 26, 1963.

3. NASA Memorandum from EG23/Systems Analysis Branch to EG/Chief, Guidance and Control Division, "Results of Study to Determine Limits of Pilot Controlled Landing Touchdown Velocities of LEM Spacecraft," dated August 14, 1964.

APPENDIX A

EQUATIONS OF MOTION

The derivation of the equations of motion of a rigid body may be found in several texts on elementary mechanics and are therefore presented herein without derivation.

DIRECTION COSINES

$l_1 = \cos\theta \cos\psi$

$l_2 = \sin\psi$

$l_3 = -\sin\theta \cos\psi$

$m_1 = \sin\theta \sin\phi - \cos\theta \sin\psi \cos\phi$

$m_2 = \cos\psi \cos\phi$

$m_3 = \cos\theta \sin\phi + \sin\theta \sin\psi \cos\phi$

$n_1 = \sin\theta \cos\phi + \cos\theta \sin\psi \sin\phi$

$n_2 = -\cos\psi \sin\phi$

$n_3 = \cos\theta \cos\phi - \sin\theta \sin\psi \sin\phi$

$a_1 = \cos\lambda$

$a_2 = 0$

$a_3 = -\sin\lambda$

$b_1 = \sin\lambda \sin L$

$b_2 = \cos L$

$b_3 = \cos\lambda \sin L$

$c_1 = \sin\lambda \cos L$

$c_2 = -\sin L$

$c_3 = \cos\lambda \cos L$

APPLIED FORCES IN THE BODY FRAME

$$a_x = \frac{\delta_\theta T_m}{M_T}, \quad a_y = \frac{-\delta_\phi T_m}{M_T}, \quad a_z = \frac{-T_m}{M_T}$$

INERTIAL VELOCITIES

$$V_{X_I} = a_x l_1 + a_y m_2 + a_z n_2 + \left(1 - \frac{2h}{R_m}\right) g_m C_1$$

$$V_{Y_I} = a_x l_2 + a_y m_2 + a_z n_2 + \left(1 - \frac{2h}{R_m}\right) g_m C_2$$

$$V_{Z_I} = a_x l_3 + a_y m_3 + a_z n_3 + \left(1 - \frac{2h}{R_m}\right) g_m C_3$$

INERTIAL POSITION

$$\dot{X}_I = V_{X_I}, \quad \dot{Y}_I = V_{Y_I}, \quad \dot{Z}_I = V_{Z_I}$$

VELOCITIES IN THE "G" FRAME

$$V_{X_G} = V_{X_I} a_1 + V_{Y_I} a_2 + V_{Z_I} a_3$$

$$V_{Y_G} = V_{X_I} b_1 + V_{Y_I} b_2 + V_{Z_I} b_3$$

$$V_{Z_G} = V_{X_I} c_1 + V_{Y_I} c_2 + V_{Z_I} c_3$$

VELOCITIES IN THE BODY FRAME

$$u = V_{X_I} l_1 + V_{Y_I} l_2 + V_{Z_I} l_3$$

$$v = V_{X_I} m_1 + V_{Y_I} m_2 + V_{Z_I} m_3$$

$$2 = V_{X_I} n_1 + V_{Y_I} n_2 + V_{Z_I} n_3$$

POSITION IN THE "G" FRAME

$$\dot{L} = \frac{V_{Y_G}}{R_m} - \frac{h\, V_{Y_G}}{R_m^2}$$

$$\dot{\lambda} = -\frac{V_{X_G}}{R_m \cos L} + \frac{h\, V_{X_G}}{R_m^2 \cos L}$$

$$\dot{h} = -V_{Z_G}$$

APPLIED MOMENTS IN THE BODY FRAME

$$L = M_\theta + T_m (Z_1 \delta_\phi + Y_1)$$

$$M = M_\theta - T_m (X_1 - Z_1 \delta_\theta)$$

$$N = M + T_m (X_1 \delta_\phi + Y_1 \delta_\theta)$$

BODY ANGULAR RATES

$$\dot{p} = \frac{1}{I_x}\left[L - (I_z - I_y)\, q\, r + I_{Y_Z} (q^2 - r^2) + I_{X_Z} (\dot{r} + pq) + I_{X_Y} (\dot{q} - pr) + p\dot{m}_m l_z^2 \right]$$

$$\dot{q} = \frac{1}{I_Y}\left[M - (I_x - I_z)\, p\, r + I_{X_Z} (r^2 - p^2) + I_{X_Y} (\dot{p} + qr) + I_{Y_Z} (\dot{r} - pq) + q\dot{m}_m l_z^2 \right]$$

$$\dot{r} = \frac{1}{I_z}\left[N - (I_y - I_x)\, p\, q + I_{X_Y} (p^2 - q^2) + I_{X_Z} (\dot{p} - qr) + I_{Y_Z} (\dot{q} + pr) + r\dot{m}_m l_{xy}^2 \right]$$

EULER ANGLES (θ, Ψ, ϕ)

$$\dot{\theta} = \frac{q \cos \phi - r \sin \phi}{\cos}$$

$$\dot{\Psi} = r \cos \phi + q \sin \phi$$

$$\dot{\phi} = p - \dot{\theta} \sin$$

PHYSICAL QUANTITIES

$$\Delta M_m = K_1 \int_o^t T_m \, dt \qquad \text{note: } \dot{M}_m = - K_1 T_m$$

$$\Delta M_{RCS} = K_2 \int_o^t (M_\theta + K_3 M_\psi + M_\phi) \, dt$$

The physical quantities at any time (t) are:

$$M_{T(t)} = M_{T(o)} - M_m - M_{RCS}$$

$$I_{X(t)} = I_{X(o)} - M_{m(t)} K_4$$

$$I_{Y(t)} = I_{Y(o)} - M_{m(t)} K_5$$

$$I_{Z(t)} = I_{Z(o)} - M_{m(t)} K_6$$

$$I_{XZ(t)} = I_{XZ(o)} + M_{m(t)} K_7$$

$$I_{XY(t)} = I_{XY(o)} + M_{m(t)} K_8$$

$$I_{YZ(t)} = I_{YZ(o)} - M_{m(t)} K_9$$

$$X_{1(t)} = X_{1(o)} + M_{m(t)} K_{10}$$

$$Y_{1(t)} = Y_{1(o)} - M_{m(t)} K_{11}$$

$$Z_{1(t)} = Z_{1(o)} + M_{m(t)} K_{12}$$

DISPLAY VELOCITIES

Inertial (with ψ transformation)

$$V_{X_D} = V_{X_I} \cos\psi + V_{Y_I} \sin\psi$$

$$V_{Y_D} = -V_{X_I} \sin\psi + V_{Y_I} \cos\psi$$

$$V_{Z_D} = V_{Z_I}$$

Radar #1 (σ transformation)

$$u_{r_1} = u \cos\sigma_R + w \sin\sigma_R$$

$$v_{r_1} = v$$

$$w_{r_1} = -u \sin\sigma_R + w \cos\sigma_R$$

σ_R = cons't

Radar #2 (body)

$$u_{r_2} = u$$

$$v_{r_2} = v$$

$$w_{r_2} = w$$

Ground range

$$R_T = \left[X_I^2 + Y_I^2 \right]^{\frac{1}{2}}$$

INITIAL CONDITIONS

t, V_{X_I}, V_{Y_I}, V_{Z_I}, X_I, Y_I, Z_I, λ, L, h

θ, ψ, ϕ, p q r

PHYSICAL QUANTITY INPUTS

M_T, M_m, I_x, I_y, I_z, I_{xy}, I_{xz}, I_{yz}, X_1, Y_1, Z_1

Constants: l_z, l_{xy}

CONTROL INPUTS

Grim gimbal $\delta\theta$, $\delta\phi$

Attitude control M_ϕ, M_θ, M_ψ

Main engine T_m

ADDITIONAL CONSTANTS

R_m, g_m, σ_R

TABLE 1.-CONTROL GAIN CONSTANTS USED IN THE FOUR CONTROL MODE CONFIGURATIONS

CONFIG-URATION	MODE	C_1	C_2
1	DIRECT THRUST CONTROL	0	0
2	LINEAR $\dot{h}$ FEEDBACK	66	66
3	NONLINEAR $\dot{h}$ FEEDBACK	194	23
4	INCREMENTAL	194	194

TABLE 2.-PILOT COOPER RATING OF THE FOUR CONTROL MODE CONFIGURATIONS

Subject	Mode 1	Mode 2	Mode 3	Mode 4
1	4.0	4.0	4.0	1.0
2	5.5	2.5	2.7	2.0
3	3.5	3.0	3.0	1.5
4	3.5	2.5	3.0	2.0
Average	4.1	3.0	3.2	1.6

Note:

Mode 1 Direct thrust control
Mode 2 Linear $\dot{h}$ feedback
Mode 3 Nonlinear $\dot{h}$ feedback
Mode 4 Incremental

TABLE 3.-MEAN AND 3σ VALUES OF TASK PARAMETERS FOR THE FOUR RATE OF DESCENT CONTROL MODES

Task Parameter	Units		Mode 1	Mode 2	Mode 3	Mode 4
V_{X_I}	ft/sec	mean	.07	.25	-.05	-.66
		3σ	3.21	3.12	3.00	2.82
V_{Y_I}	ft/sec	mean	-.90	-1.00	-.90	-.44
		3σ	4.20	3.90	2.64	3.00
V_{Z_I}	ft/sec	mean	5.00	4.30	4.30	5.20
		3σ	5.70	4.20	3.90	2.01
θ	deg.	mean	-.58	-.27	-.29	-.07
		3σ	2.97	6.60	5.10	2.58
ψ	deg.	mean	.25	-.12	-.68	-.93
		3σ	4.20	2.76	2.43	2.28
ϕ	deg.	mean	.89	.84	1.20	1.10
		3σ	3.30	3.93	3.90	2.04
X_I	ft.	mean	-128	-44	-73	-59
		3σ	333	306	387	261
Y_I	ft.	mean	-66	-81	-57	-35
		3σ	243	183	216	153
q	deg/sec	mean	.00	-.14	-.02	.05
		3σ	.21	1.77	.30	.21
r	deg/sec	mean	-.03	.00	-.03	.00
		3σ	.09	.18	.15	.06
p	deg/sec	mean	-.05	-.07	-.05	.01
		3σ	.45	.42	.60	.15

Note:

Mode 1 Direct thrust control
Mode 2 Linear $\dot{h}$ feedback
Mode 3 Nonlinear $\dot{h}$ feedback
Mode 4 Incremental

TABLE 4.-MEAN AND 3 σ VALUES OF NON-TASK PARAMETERS FOR THE FOUR RATE OF DESCENT CONTROL MODES

Nontask Parameters	Units		Model 1	Model 2	Model 3	Model 4
t*	sec.	mean	125	125	118	122
		3 σ	42	45	102	42
Δ V**	ft/sec	mean	744	745	750	732
		3 σ	222	231	222	219
W_{RCS}	lbs.	mean	42	44	45	32
		3 σ	36	39	39	54
M_m	slugs	mean	418	418	418	416
		3 σ	10	10	10	11

*Includes 15 seconds of automatic control

**Includes 142 ft/sec characteristic velocity expended during automatic control

Note:

Mode 1 Direct thrust control
Mode 2 Linear $\dot{h}$ feedback
Mode 3 Nonlinear $\dot{h}$ feedback
Mode 4 Incremental

TABLE 5.-CONTROL MODE RELATIVE GRADING

Task Parameter	Mode 1	Mode 2	Mode 3	Mode 4
X_I	4	1	3	2
Y_I	4	2	3	1
V_{X_I}	2	3	1	4
V_{Y_I}	4	3	2	1
V_{Z_I}	4	3	2	1
θ	2	4	3	1
ψ	4	1	2	3
ϕ	2	3	4	1
total	26	20	20	14

Nontask Parameter	Mode 1	Mode 2	Mode 3	Mode 4
t	2	3	4	1
ΔV	2	4	3	1
W_{RCS}	1	2	3	4
total	5	9	10	6

Note:

Mode 1 Direct thrust control
Mode 2 Linear $\dot{h}$ feedback
Mode 3 Nonlinear $\dot{h}$ feedback
Mode 4 Incremental

TABLE 6.-PILOT COOPER RATING OF FOUR ATTITUDE HOLD ENGAGEMENT RATES

	Attitude hold engagement rate - deg/sec			
Subject	1	2	3	5
1	3.2	3.5	3.7	4.0
2	3.5	3.5	4.0	5.0
3	3.6	3.8	4.0	5.0
4	3.2	3.4	3.5	4.5
Average	3.4	3.5	3.8	4.6

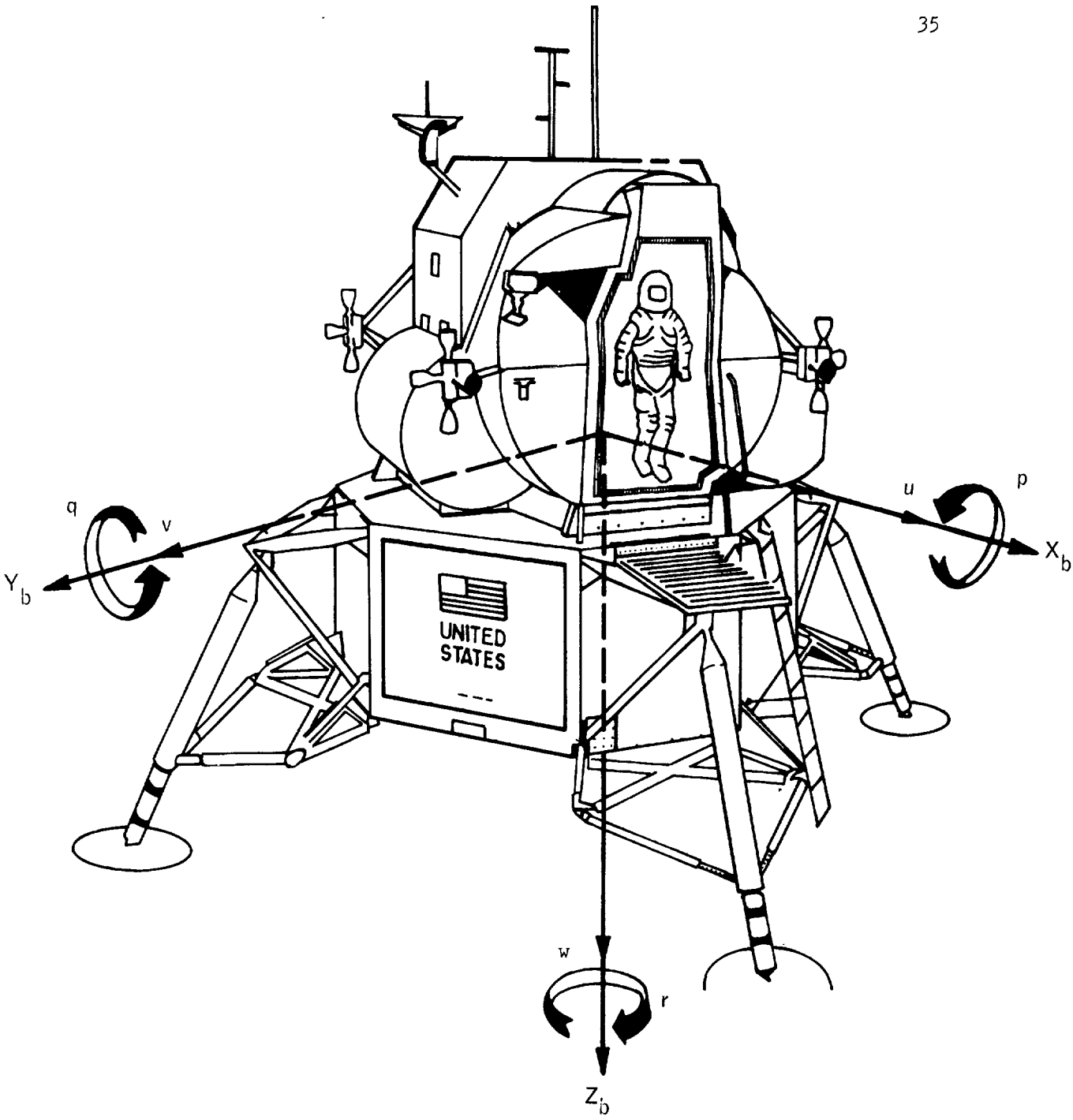

Figure 1.- General configuration of simulated vehicle.

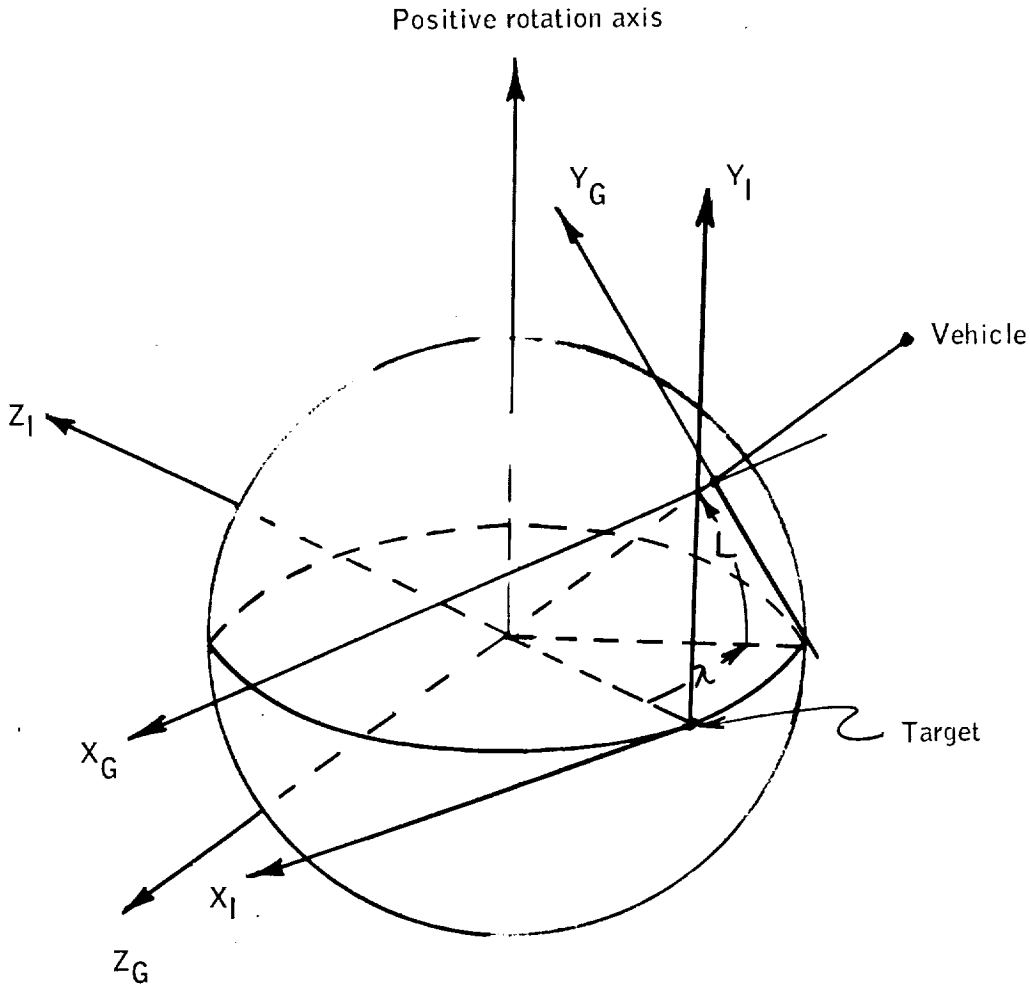

Figure 2.- Lunar axes systems.

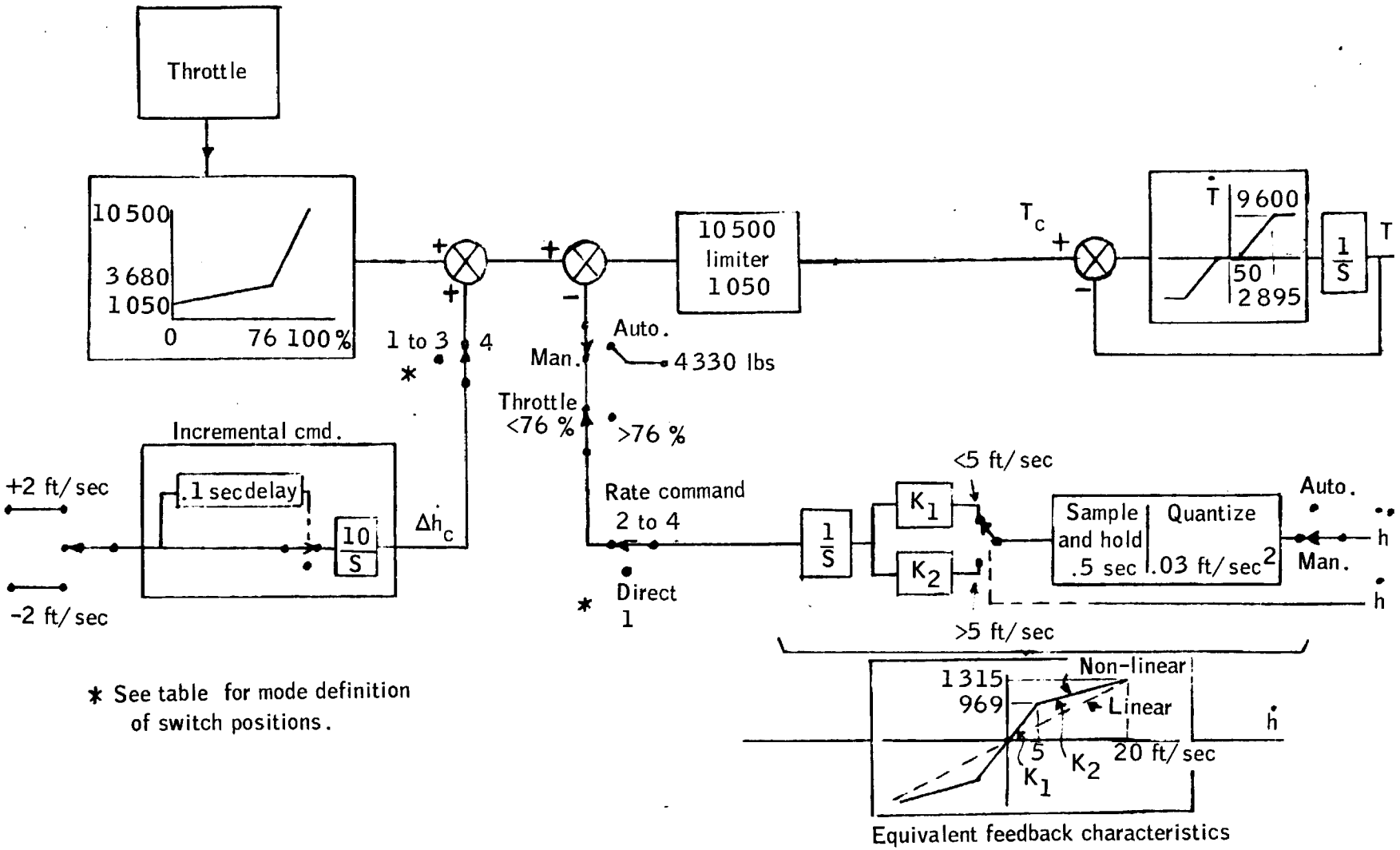

Figure 3.- Rate of descent control systems.

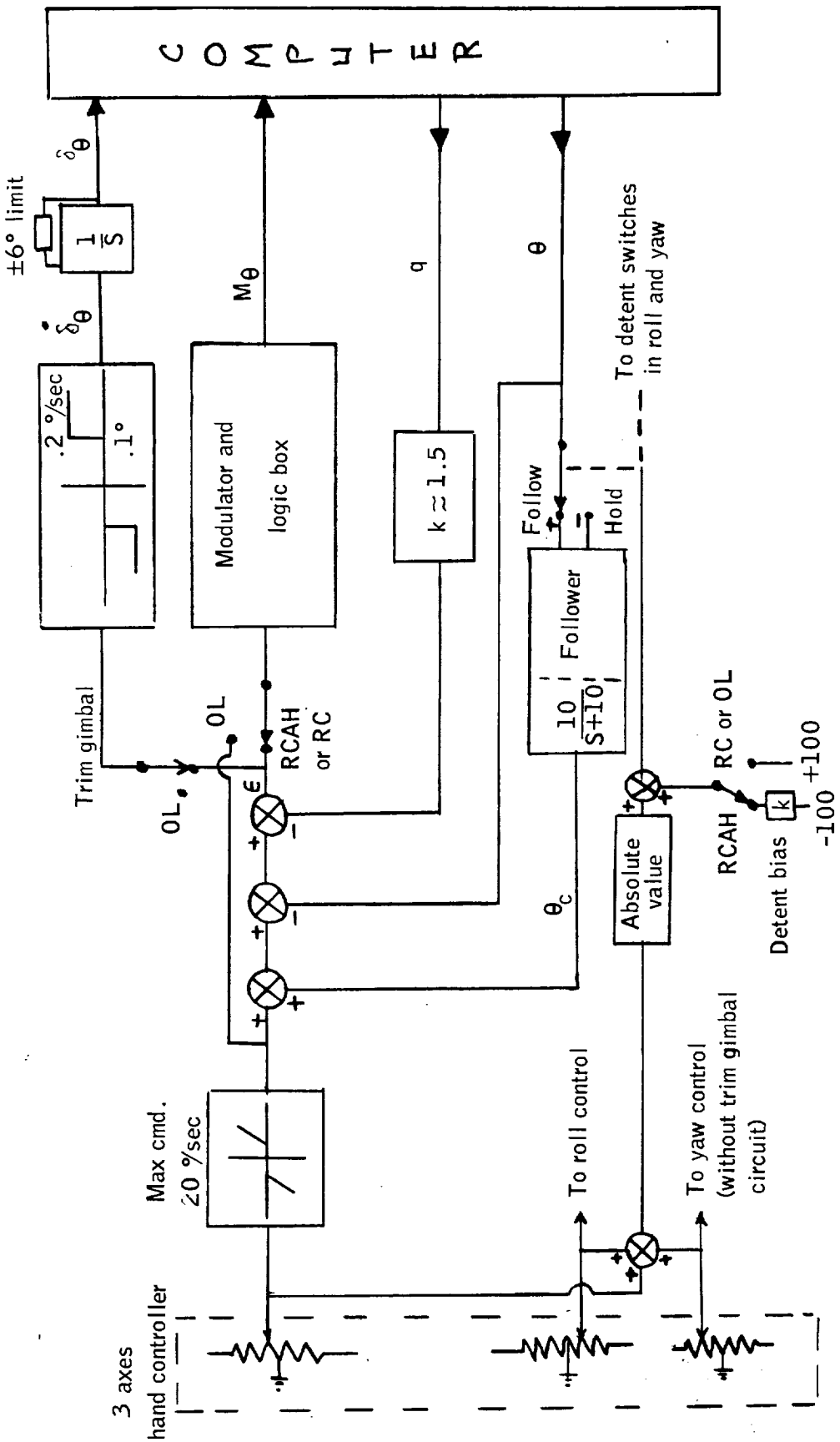

Figure 4.- Attitude control system for pitch axis.

NASA
S-64-29366

Figure 5.- Hand controller.

NASA
S-64-29367

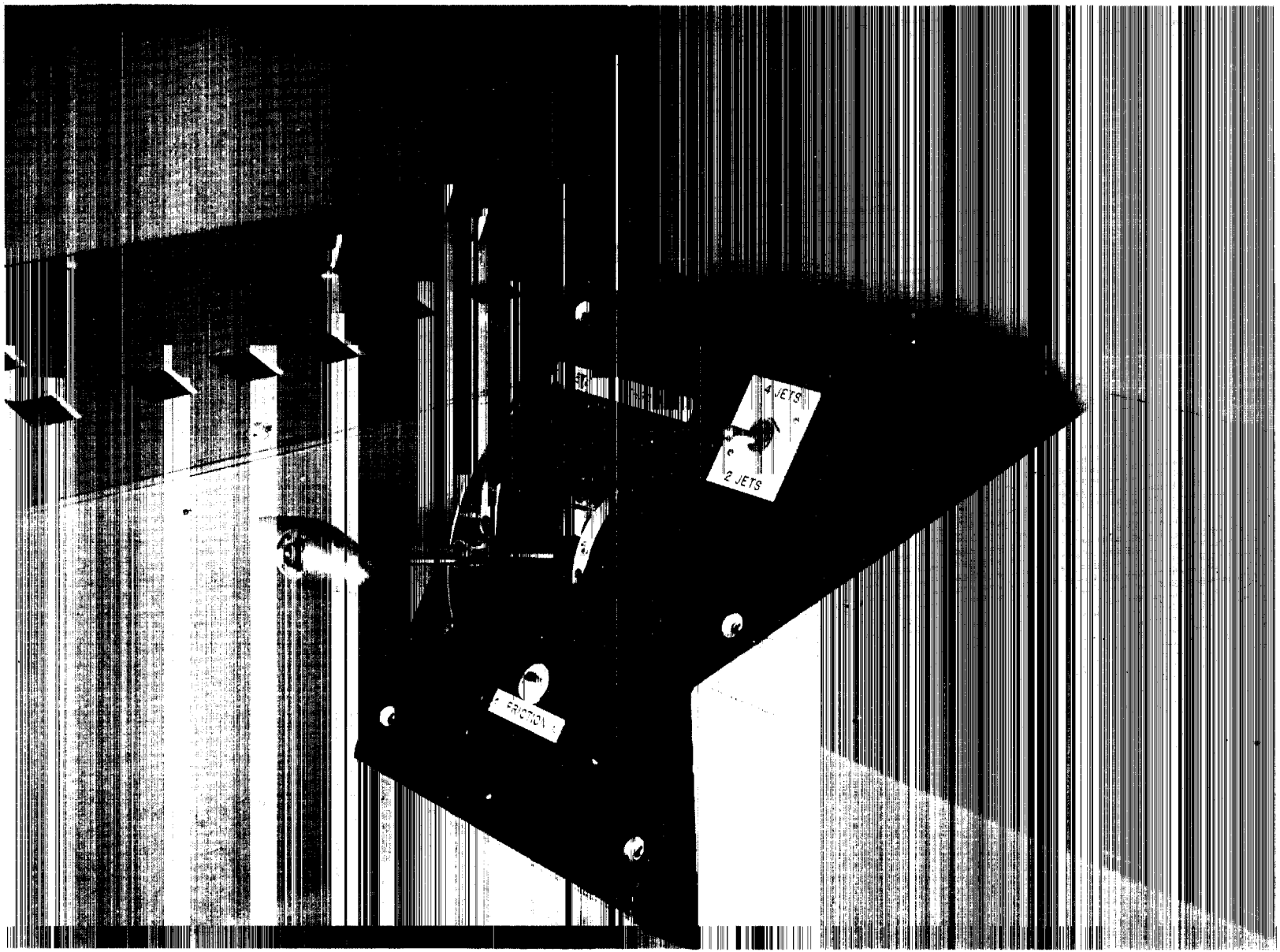

Figure 6.- Main engine throttle

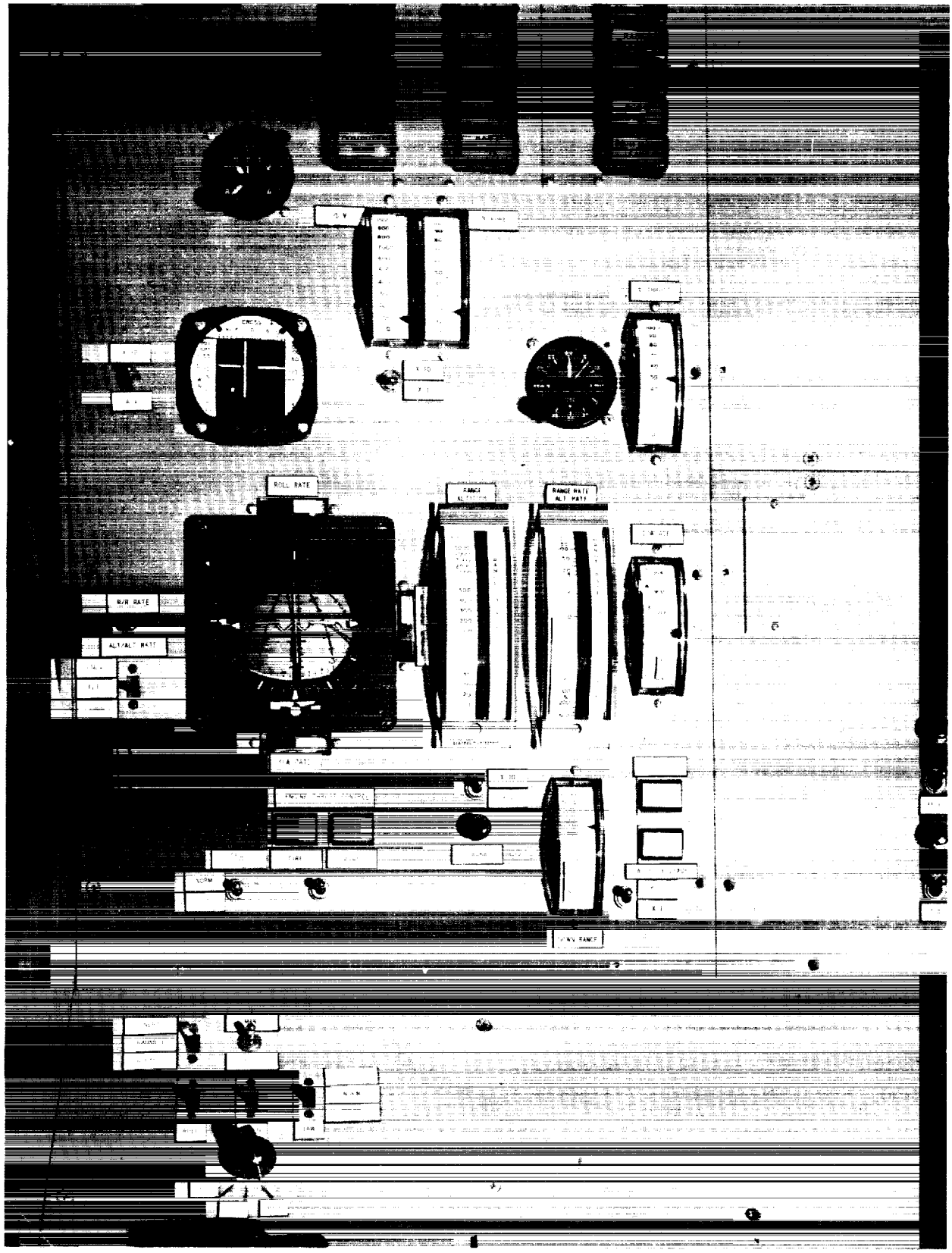

NASA S-64-39009

(a) Command astronaut panel.

Figure 7.- Flight display panel used in the simulation.

MSC 5739-65

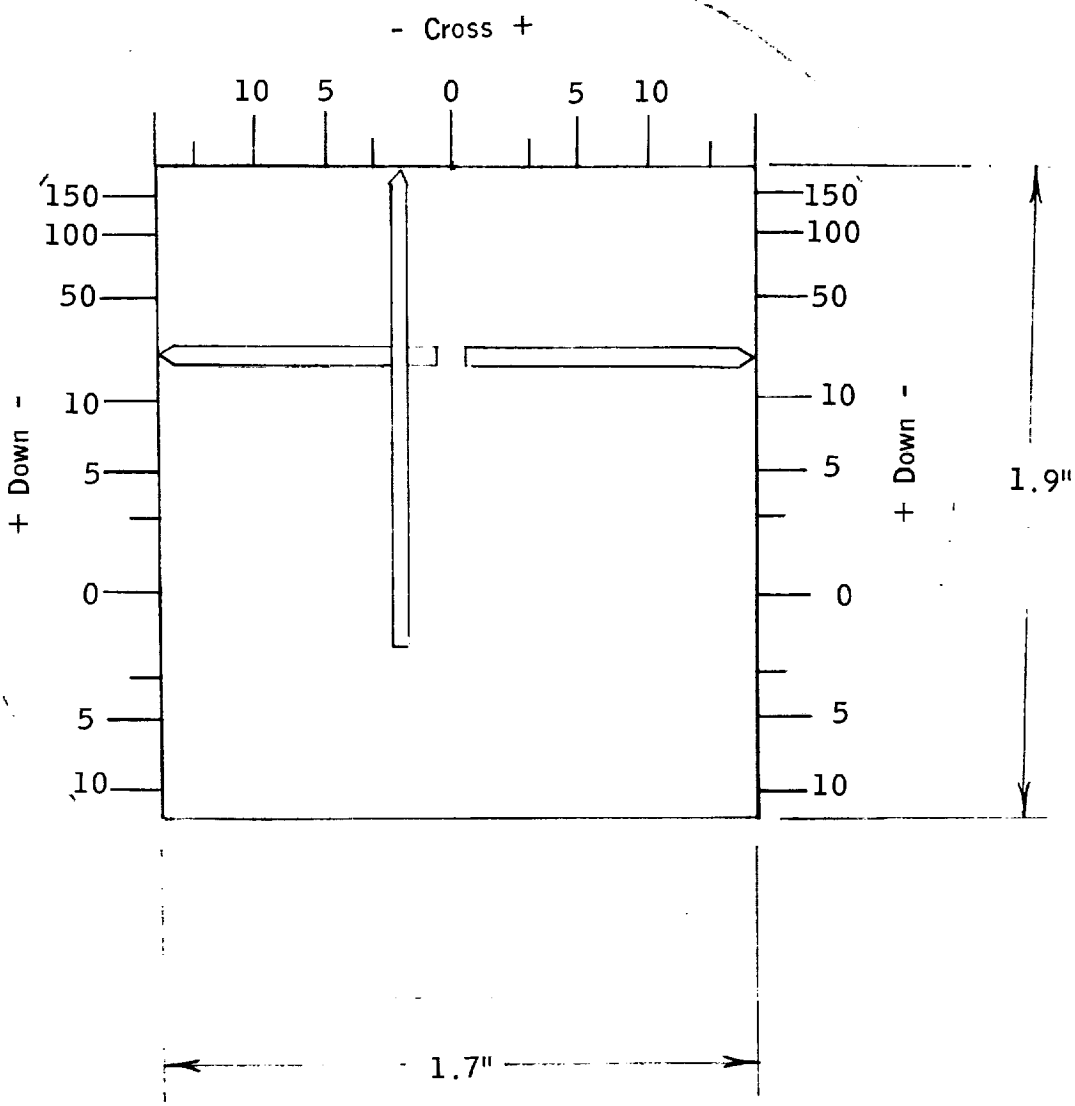

Note: Scale 2" = 1".

(b) Forward and lateral velocity indicator.

Figure 7.- Concluded.